

Velocity Distribution Function of a Streaming Gas via Nonequilibrium Molecular Dynamics

Werner Loose and Siegfried Hess

Institut für Theoretische Physik, Technische Universität Berlin, D-1000 Berlin 12, West Germany

(Received 9 March 1987)

The shear-flow-induced distortion of the velocity distribution function of a Lennard-Jones gas is computed in a nonequilibrium molecular-dynamics simulation and compared with the kinetic theory based on the Boltzmann equation.

PACS numbers: 51.10.+y, 05.20.Dd, 61.20.Ja

The velocity distribution function of a nonequilibrium fluid deviates from the Maxwellian equilibrium distribution. Since transport coefficients are related to integrals over the distorted velocity distribution, it plays a central role in the kinetic theory which, for dilute gases, is based on the Boltzmann equation.¹ A direct test of the theory on the level of the distribution function rather than via the transport coefficients is desirable but experimentally difficult.² Nonequilibrium molecular dynamics can provide the wanted data for specific model systems. Here, computer simulation results are reported for a moderately dense Lennard-Jones gas undergoing a plane Couette flow (simple shear). A comparison with kinetic theory is made. The present work extends previous studies on the shear-flow-induced distortion of the pair-correlation function of dense fluids.³

The distribution of the velocities \mathbf{c} of particles (with mass m) of a fluid with density n is described by the velocity distribution function $f(\mathbf{c})$. The standard normalization is $\int f d^3c = n$. For convenience, the dimensionless peculiar velocity \mathbf{V} is introduced by

$$\sqrt{2}c_0\mathbf{V} = \mathbf{c} - \mathbf{v}, \quad (1)$$

where \mathbf{v} is the (local) average flow velocity and $c_0 = (k_B T/m)^{1/2}$ is a thermal reference velocity; T is the temperature. In the following, the velocity distribution is characterized by the function $F(\mathbf{V})$ related to $f(\mathbf{c})$ by

$$nF(\mathbf{V})d^3V = f(\mathbf{c})d^3c. \quad (2)$$

Notice that $\int F d^3V = 1$. The possible dependence of n , \mathbf{v} , \mathbf{V} , T , f , and F on the time t and the position \mathbf{r} has not been indicated explicitly.

The function $F(\mathbf{V})$ can be expanded with respect to basis functions, e.g., spherical harmonics $Y_{lm}(\hat{\mathbf{V}})$ or Cartesian tensors constructed from the components of the unit vector $\hat{\mathbf{V}} = V^{-1}\mathbf{V}$. The expansion "coefficients" then are functions of the magnitude $V = |\mathbf{V}|$ of the velocity. For the special case of a plane Couette flow with the flow velocity \mathbf{v} in the x direction and its gradient in the y direction, the expansion reads

$$F(\mathbf{V}) = F_s + F^{(21)}\hat{V}_x\hat{V}_y + F^{(22)}\frac{1}{2}(\hat{V}_x^2 - \hat{V}_y^2) + F^{(20)}(\hat{V}_z^2 - \frac{1}{3}) + \dots \quad (3)$$

The "scalar" part $F_s(V)$ is the directional average of $F(\mathbf{V})$,

$$F_s = (4\pi)^{-1} \int F(\mathbf{V})d^2\hat{V}, \quad (4)$$

where $d^2\hat{V}$ stands for the solid-angle element. Similarly, the three second-rank tensorial functions $F^{(2k)}$, $k=0,1,2$, are weighted directional averages of $F(\mathbf{V})$,

$$F^{(2k)} = (4\pi)^{-1} \times \frac{15}{2} \int Y_k(\hat{\mathbf{V}})F(\mathbf{V})d^2\hat{V}, \quad (5)$$

with

$$Y_1 = 2\hat{V}_x\hat{V}_y, \quad Y_2 = (\hat{V}_x^2 - \hat{V}_y^2), \quad Y_0 = \frac{3}{2}(\hat{V}_z^2 - \frac{1}{3}).$$

The dots in (3) stand for terms involving tensors of ranks $l \geq 4$.

In (local) thermal equilibrium, F_s reduces to the (local) Maxwellian $F_M = \pi^{-3/2} \exp(-V^2)$ and all other terms vanish in the expansion (3). An integral over the function $F^{(21)}$ yields the x,y element of the pressure tensor and is thus related to the (non-Newtonian) viscosity η_+ by

$$P_{xy} = \frac{8\pi}{15} P \int_0^\infty F^{(21)} V^4 dV = -\eta_+ \gamma. \quad (6)$$

Here, $\gamma = \partial v_x / \partial y$ is the (constant) shear rate and $P = nk_B T$ is the ideal-gas pressure. Clearly, $\gamma \eta_+ \neq 0$ implies $F^{(21)} \neq 0$. Similar relations for the normal pressure differences involve $F^{(22)}$ and $F^{(20)}$ and coefficients η_- and η_0 .^{3,4} Next, the partial distributions F_s and $F^{(21)}$ are presented as functions of V^2 as inferred from a molecular-dynamics simulation.

Newton's equations of motions of N particles in a box with volume V (determined by the number densities $n = N/V$) are integrated numerically (fifth-order Gear predictor-corrector method with a time step $\Delta t = 0.005$); periodic boundary conditions are employed and constraints are imposed to simulate a thermostat (rescaling of the velocities) and the linear velocity profile of a plane Couette flow (homogeneous shear algorithm⁴). The main differences as compared with earlier studies^{3,5-7} are the use of vectorized algorithms in order to take advantage of the computing capabilities of a Cray Research (1-M; more recently, X-MP) computer and, of course, the extraction of the additional data needed for

the velocity distribution function. More specifically, the quantities $F_s, F^{(21)}, F^{(22)}, F^{(20)}$ of Eq. (3) are the N -particle averages of

$$\sum_i \delta(V - V_i), \quad \sum_i \hat{V}_x \hat{V}_y \delta(V - V_i),$$

$$\sum_i \frac{1}{2} (\hat{V}_x^2 - \hat{V}_y^2) \delta(V - V_i), \quad \sum_i (\hat{V}_z^2 - \frac{1}{3}) \delta(V - V_i),$$

respectively. In the calculation, the velocity space is divided into 64 spherical shells chosen such that the average number of particles, proportional to $V^2 \exp(-V^2)$, is about equal in each of them. This implies that the intervals are broader for low speeds ($V^2 < 0.2$) and high speeds ($V^2 > 2.5$).

The binary Lennard-Jones potential $\phi = 4\epsilon[(\sigma/r)^{12} - (\sigma/r)^6]$ (cut off at $r = 2.5\sigma$) is used to model the particle interaction. Characteristic scales for the energy and the length are provided by ϵ and σ , respectively. Density, temperature, and shear rate are expressed in reduced units, i.e.,

$$n = n^* \sigma^{-3}, \quad T = T^* \epsilon / k_B, \quad \gamma = \gamma^* \sigma^{-1} (\epsilon / m)^{1/2},$$

where m is the mass of a particle. In the following the asterisks are dropped for convenience. The data presented are for the temperature $T = 1.2$ and the number density $n = 0.07$; further data are also available for $T = 2.75$ at the number densities $n = 0.1$ and $n = 0.01$. The simulation was performed for $N = 8^3 = 512$ particles; time averages are over 32 consecutive runs of 5000 time steps (or a total of 160000 time steps).

Figure 1 shows the scalar part F_s of the velocity distribution as function of V^2 for $T = 1.2, n = 0.07$ and the shear rate $\gamma = 0.06$ as extracted from the simulation: a practically perfect Maxwellian distribution, $F_s \approx F_M$. The normalization and the temperature calculated with this velocity distribution agree with the expected values to better than 0.1%. The straight line corresponds to the computed $\ln F_s \sim -V^2$ (right scale).

In Fig. 2, $F^{(21)}$ is displayed as function of V^2 for the same state point and the shear rate $\gamma = 0.06$. The curves

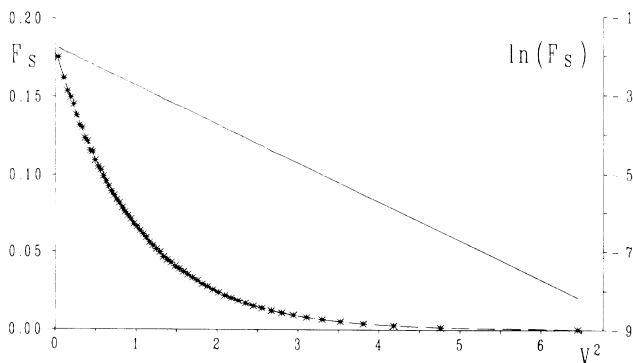


FIG. 1. The scalar part F_s of the velocity distribution and $\ln F_s$ as functions of V^2 . The logarithmic scale is indicated on the right-hand side.

shown in Figs. 2 and 3 stem from kinetic theory. The asterisks mark the computed averages; the vertical lines indicate the statistical error. It should be pointed out that the integral (6) over $F^{(21)}$ yields a value of the viscosity η_+ which is just about 1% larger than the value evaluated directly from the N -particle average of the x, y element of the kinetic part of the pressure tensor. Obviously, the errors for small velocities do not affect the viscosity which is mainly determined by the faster particles.

Figure 3 shows the same shear-flow-induced distortion now presented via the ratio $F^{(21)}/F_M$. Clearly, if one divides by the number of particles present in the velocity shells, the relative errors of the data points are smaller.

Kinetic theory, based on the Boltzmann equation, yields for the present problem,^{1,8,9}

$$F^{(21)} = F_M [-2(\eta_+ / nT) \gamma V^2 + \dots], \quad (7)$$

where η_+ is the non-Newtonian viscosity and the ellipsis stands for terms involving higher Sonine polynomials. In the linear flow regime, η_+ reduces to the Newtonian (kinetic) viscosity $nT\tau$ with the relaxation time τ , determined by collision integrals,¹ being equal to 1.58 (in Lennard-Jones units) for a Lennard-Jones gas at the state point chosen. The linear approximation $F^{(21)} = -2\gamma\tau V^2 F_M$ yields the curve shown in Fig. 2 and the straight line in Fig. 3. As expected from kinetic theory the role of the higher Sonine polynomials is not important for $\gamma\tau \lesssim 0.1$. The comparison between theory and computer simulation data which does not involve any adjustable parameter is excellent for small shear rates.

At higher shear rates ($\gamma\tau \gtrsim 0.1$) a number of deviations from the simple linear theory are expected. The viscosity η_+ occurring in (7) depends on the shear rate; the normal pressure differences $P_{xx} - P_{yy}$ and $P_{zz} - \frac{1}{2}(P_{xx} + P_{yy})$, characterized by the viscosity coefficients η_- and η_0 , respectively,^{5,8} are nonzero and consequently the closely related functions $F^{(22)}$ and $F^{(20)}$ of

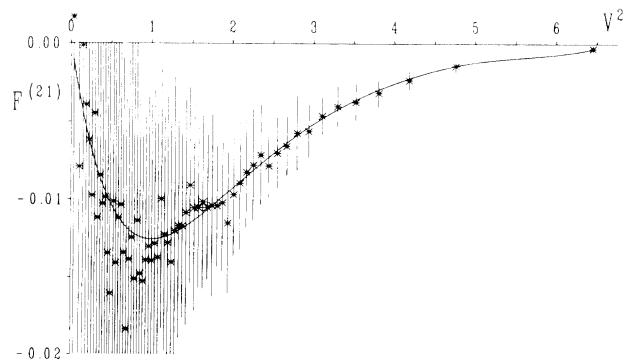


FIG. 2. The (partial) distribution function $F^{(21)}$ for the shear rate $\gamma = 0.06$ obtained from the simulation as function of V^2 . The statistical error is indicated by the vertical lines.

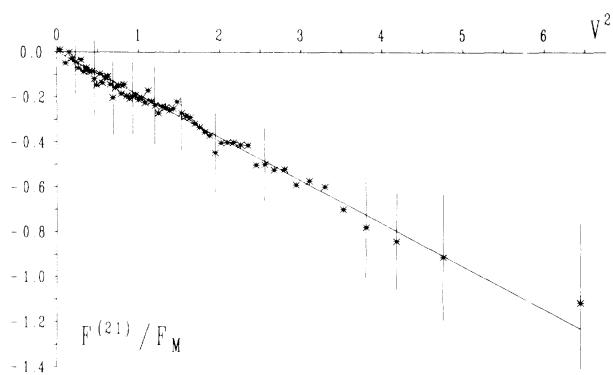


FIG. 3. The partial distribution function $F^{(21)}$ of Fig. 2 divided by the Maxwellian distribution [see Eq. (7)]. The straight line corresponds to the result of the linear approximation, $F^{(21)}/F_M = -2\gamma\tau V^2$; for $\gamma=0.06$, $T=1.2$, $n=0.07$, and $\gamma\tau=0.095$.

Eq. (3) can be observed in the molecular-dynamics simulation in analogy to $F^{(21)}$. Two less obvious nonlinear features are the increasing importance of the Sonine-polynomial contributions indicated by the ellipsis in (7) with increasing shear rate and the deviation of F_s from the Maxwellian F_M . The moment-method solution of the Boltzmann equation presented in Ref. 8 gives good results when applied to the nonlinear flow behavior characterized by the viscosity coefficients.^{5,9} The comparison with the velocity distribution function, however, requires an extended set of moments. The simplest relevant extension yields the observed nonlinear phenomena.⁹

It has been demonstrated that nonequilibrium molecular dynamics can be applied successfully to study the shear-flow-induced distortion of the velocity distribution function of a gas. Excellent agreement with the kinetic theory based on the Boltzmann equation is found in the linear flow regime. This may be looked upon as a quasiexperimental verification of the kinetic theory on

the level of the distribution function or, alternatively, as a test of the quality of the nonequilibrium molecular-dynamics simulation.

An enthusiastic plea for the computation of the velocity distribution function via nonequilibrium molecular dynamics was presented to one of us (S.H.) by F.R. McCourt. This led to first feasibility studies run on the Digital Equipment Corporation PDP-10 computer of the Institut Max von Laue-Paul Langevin in Grenoble, France. Calculations with sufficient statistical accuracy as presented here were performed on the Cray Research (1-M, X-MP) computers of the Zentrum für Informationstechnik Berlin.

¹S. Chapman and T. G. Cowling, *The Mathematical Theory of Nonuniform Gases* (Cambridge Univ. Press, Cambridge, England, 1939); L. Waldmann, in *Handbuch der Physik*, edited by S. Flügge (Springer-Verlag, Berlin, 1958), Vol. 12; *The Boltzmann Equation, Theory and Applications*, edited by E. G. D. Cohen and W. Thirring (Springer-Verlag, Wien, 1973).

²Measurements of the heat-flow-induced distortion of the velocity distribution are presented in F. Baas, P. Oudemans, H. F. P. Knaap, and J. J. M. Beenakker, *Physica (Amsterdam)* **89A**, 73 (1977); B. S. Douma, H. F. P. Knaap, and J. J. M. Beenakker, *Chem. Phys. Lett.* **74**, 421 (1980).

³D. J. Evans, H. J. M. Hanley, and S. Hess, *Phys. Today* **37**, No. 1, 26 (1984); S. Hess and H. J. M. Hanley, *Phys. Rev. A* **25**, 1801 (1982); S. Hess, *Int. J. Thermophys.* **6**, 657 (1985).

⁴D. J. Evans, *Mol. Phys.* **37**, 1745 (1979).

⁵S. Hess, H. J. M. Hanley, and N. Herdegen, *Phys. Lett.* **105A**, 238 (1984).

⁶S. Hess, *J. Mec. Theor. Appl.*, Numéro Spécial 1985, edited by D. Quemada, p. 1.

⁷D. Baalss and S. Hess, *Phys. Rev. Lett.* **57**, 86 (1986).

⁸N. Herdegen and S. Hess, *Physica (Amsterdam)* **115A**, 281 (1982).

⁹W. Loose, Diplomarbeit, Technische Universität Berlin, 1986 (unpublished).